Chinese Chemical Letters 33 (2022) 2052–2056

Contents lists available at ScienceDirect

Chinese Chemical Letters

journal homepage: www.elsevier.com/locate/cclet

DNA origami-based nano-hunter enriches low-abundance point mutations by targeting wild-type gene segments

Longjie Li[a,b,1,*], Kejun Dong[c,d,1], Xinyu Wang[e], Meizhou Zhang[b], Jun Li[b], Andreas K. Nussler[f], Xianjin Xiao[d], Hongbo Wang[c,**], Yuzhou Wu[b,**]

[a] School of Life Science and Technology, Wuhan Polytechnic University, Wuhan 430023, China
[b] Hubei Key Laboratory of Bioinorganic Chemistry and Materia Medica, Hubei Engineering Research Center for Biomaterials and Medical Protective Materials, School of Chemistry and Chemical Engineering, Huazhong University of Science and Technology, Wuhan 430074, China
[c] Department of Obstetrics and Gynecology, Union Hospital, Tongji Medical College, Huazhong University of Science and Technology, Wuhan 430022, China
[d] Institute of Reproductive Health, Tongji Medical College, Huazhong University of Science and Technology, Wuhan 430030, China
[e] Department of Breast Surgery, Second Hospital of Jilin University, Changchun 130041, China
[f] Siegfried Weller Institute for Trauma Research, Eberhard-Karls-Universität Tübingen, Schnarrenbergstr. 95, D-72076, Tübingen, Germany

ARTICLE INFO

Article history:
Received 7 August 2021
Revised 3 September 2021
Accepted 15 September 2021
Available online 21 September 2021

Keywords:
Low-abundance point mutation
Cancer diagnosis
DNA nano-hunter
Enrichment
Resettability

ABSTRACT

Point mutations can be used as biomarkers to perform diagnosis for diseases. In this study, a nanorobot for low-abundance point mutation enrichment was constructed using DNA origami. The novel design achieved limits of detection of 0.1% and 1% for synthesized DNA samples and clinical gene samples, respectively. Resettability was a key property of this method, which also involved a simpler process, lower cost and shorter detection duration than traditional enrichment methods. This novel DNA nanorobot may enable the detection of tumor markers, potentially facilitating early cancer diagnosis.

Point mutations are random changes in the composition or sequence of DNA base pairs at the molecular level. Many accumulated somatic point mutations can lead to diseases, including cancer [1–4]. Therefore, point mutations can be used as biomarkers that provide critical information enabling early diagnosis, real-time monitoring and treatment efficacy evaluations [5–7]. The sensitive and rapid detection of point mutations has broad prospects for research regarding the relationship between mutations and diseases and for clinical applications. However, the abundance of point mutations in the blood is too low for detection using common methods. Therefore, there is a high demand for methods that improve the accuracy and convenience of DNA-based molecular diagnoses by increasing the abundance of gene mutations in clinical samples [5,8–12].

Researchers have developed a variety of methods for the enrichment of low-abundance point mutations, such as selective polymerase chain reaction (PCR) [13–17], magnetic bead-based enrichment [18], CRISPR-Cap [19] and duplex-specific nuclease-based enrichment [20], which are highly effective and widely used. The current methods have the advantage of low detection limit, but there are some drawbacks such as complicated operation process, complex reaction components and non-specific adsorption of mutant DNA [13–20]. Therefore, to overcome these shortcomings, novel methods are needed for the enrichment of low-abundance point mutations.

Recently, DNA nanotechnology has emerged in the field of tumor recognition and treatment [21–24]. The following characteristics of DNA materials enable many biomedical applications and provide advantages over other nanomaterials: (1) the hybridization between DNA molecules, which follows the Watson-Crick complementary base-pairing principle and enables designability; (2) the size and shape of DNA nanostructures, which can be controlled *via* the DNA origami technique invented in 2006; and (3) the simplicity, efficiency and low cost of DNA synthesis and modification [23,25]. DNA nanorobots enable precise tumor treatment by identifying specific tumor-related molecules [26]. DNA nanomaterials also play an important role in tumor detection. Zhao *et al.* developed a platform by using the unique function of DNA nanomaterials to capture and isolate circulating tumor cell using three-

* Corresponding author at: School of Life Science and Technology, Wuhan Polytechnic University, Wuhan 430023, China.
** Corresponding authors.
E-mail addresses: lilongjie@whpu.edu.cn (L. Li), hb_wang1969@sina.com (H. Wang), wuyuzhou@hust.edu.cn (Y. Wu).
[1] These authors contributed equally to this work.

https://doi.org/10.1016/j.cclet.2021.09.055
1001-8417/

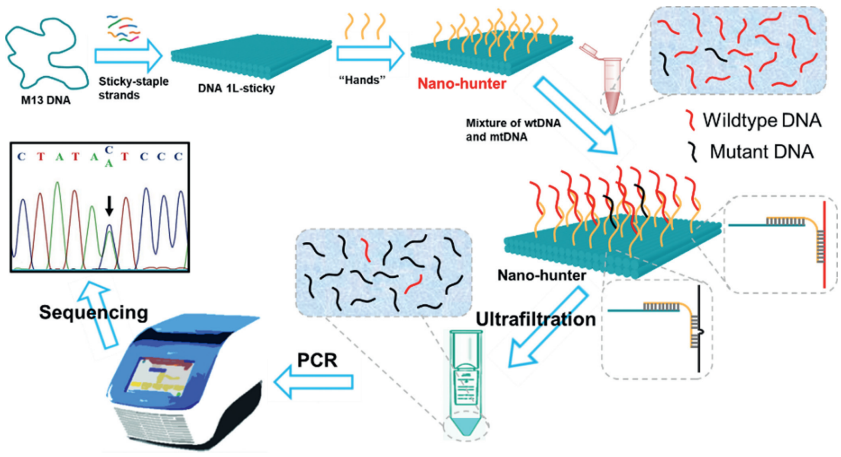

Scheme 1. Design of DNA nano-hunter for low-abundance point mutations enrichment.

dimensional (3D) DNA networks comprising repeating adhesive aptamer domains [27]. Cheng *et al.* designed an ultrasensitive sensing platform for microRNA detection based on branched DNA structures, which has broad application prospects in early diagnosis of primary cancer [28]. Therefore, we believe DNA nanotechnology is an innovative approach to enrich of low-abundance point mutations for early cancer diagnosis.

In this work, we design a DNA nanorobot capable of autonomously capturing DNA, which is called DNA nano-hunters. As shown in Scheme 1, a DNA tile of approximately 70 nm × 100 nm was created using DNA origami. It was then inserted with 180 "hands", forming a nano-hunter. They capture large amounts of interfering wild-type DNA (wtDNA) entirely by complementary base pairing. There is a base mismatch between mutant DNA (mtDNA) and nano-hunter, which leads to a decrease of their binding, so that wtDNA can be removed by ultrafiltration and mtDNA is enriched. The novel nanorobot could enrich low-abundance point mutations and thereby improve their relative abundance in clinical blood samples.

We first constructed a two-dimensional nanostructure (the 1L-sticky tile) using DNA origami (schematic shown in Fig. S1B in Supporting information) [29–31]. The 1L-sticky tile was composed of a scaffold strand and more than 200 staple strands attached *via* base pairing. The staple strands were 20 bases (7 spacers and 13 sticky ends) longer than those of the typical DNA tile structure (1L). This design simplified and reduced the cost of the screening and replacement of hand strands. Atomic force microscopy (AFM) characterization showed that the 1L-sticky tile (Fig. 1A, central panel) was approximately 0.97 nm taller than the 1L tile (Fig. 1A, left panel). We designed ten different types of hand strand (hands 10–19) to capture the wtDNA of the breast cancer susceptibility gene [*BRCA1* L771L (2430T > C)]. These different hand strands comprised 10–19 bases complementary to those of the wtDNA, and each contained one base mismatch with the mtDNA in the middle region of *BRCA1*.

We incubated the 1L-sticky tiles with each of the ten types of hand strands and performed purification, yielding ten different DNA nano-hunters. The nano-hunters were then incubated with *BRCA1* wtDNA and mtDNA, respectively. After ultrafiltration, the filtrate was collected for real-time quantitative PCR (RT-qPCR). WtDNA or mtDNA captured by nano-hunter was trapped in the upper layer of the ultrafiltration spin column *via* ultrafiltration process, and the free wtDNA or mtDNA was in the filtrate at the bottom. The hands of hunter-*n* compose *n* bases completely complementary to the wtDNA of *BRCA1* gene, while single-base mismatched with mtDNA in the middle. Therefore, the ratio of the

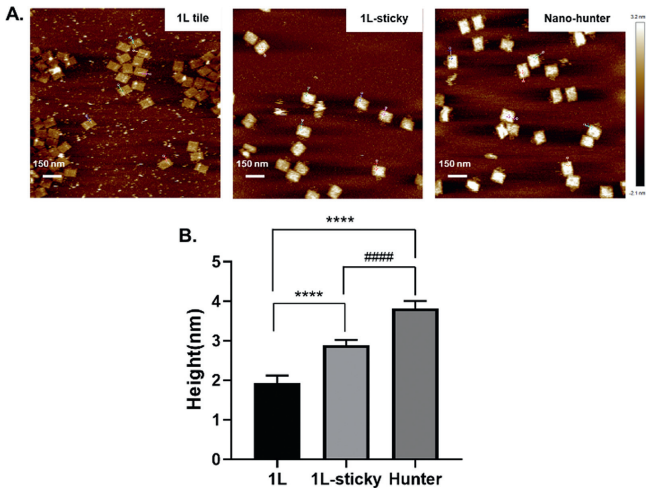

Fig. 1. AFM images (A) and height comparison (B) of 1L origami, 1L origami with sticky strands and nano-hunter. Data are represented as mean ± standard deviation (SD), $n \geq 10$. *P*-values were calculated with student's *t* test, $^{****}P < 0.0001$, $^{\#\#\#\#}P < 0.0001$.

mtDNA in the filtrate to the wtDNA in the filtrate (discrimination efficiency) would reflect the discrimination efficiency of hunter-*n*. Fig. 2A and Fig. S2 (Supporting information) illustrate that hunter-15 had the highest capture efficiency for wtDNA and a low capture efficiency for mtDNA, and the discrimination efficiency is the highest. Therefore, hunter-15 was identified as the optimal nano-hunter for *BRCA1* and used for subsequent experiments. From the data in Fig. S2, we speculate that the short hand strands are not efficient in capturing wtDNA. However, longer hand strands are not always better, as the hand strands on the surface of nano-hunter are dense and the longer hand strands may affect their binding to wtDNA. The 15 bases might be the optimal length among the 10 hands. Fig. 1A (right panel) illustrates that hunter-15 was 0.92 nm taller than the 1L-sticky tile, indicating successful assembly. The differences of the three nanostructures are significant (Fig. 1B). Meanwhile, we also demonstrated that every nano-hunter consists of about 173 hands *via* measuring the concentration of hand strands before and after mixing with 1L-sticky (Table S3 and Fig. S8 in Supporting information).

Next, we tested the capture ability of hunter-*15*. Synthetic wtDNA and mtDNA of *BRCA1* were mixed in ratios of 1:1, 9:1 and 99:1 to obtain samples with mtDNA abundances of 50%, 10% and

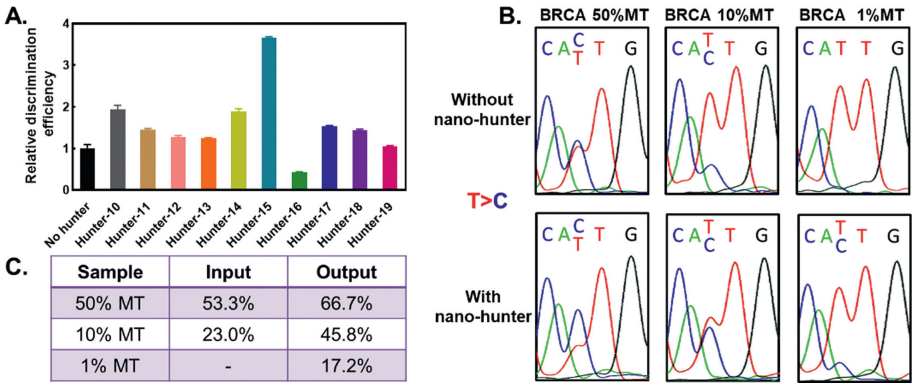

C.

Sample	Input	Output
50% MT	53.3%	66.7%
10% MT	23.0%	45.8%
1% MT	-	17.2%

Fig. 2. Nano-hunter for synthesized *BRCA1* L771L (2430T > C). (A) The capture efficiency of different nano-hunter (the efficiency of distinguishing mtDNA from wtDNA). (B) The sequencing peaks of mtDNA with different abundances before and after enrichment.

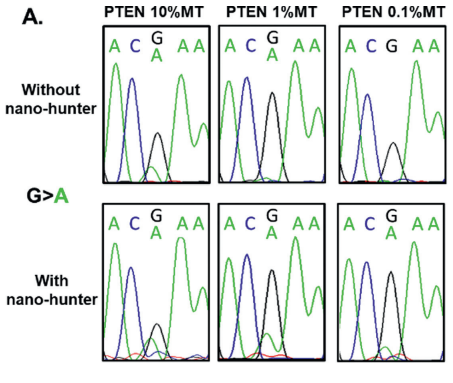

B.

Sample	Input	Output
10% MT	24.3%	37.5%
1% MT	-	22.6%
0.1% MT	-	14.3%

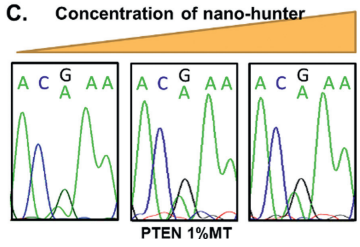

Fig. 3. Nano-hunter for synthesized *PTEN* R130Q (389G > A). (A) The sequencing peaks of mtDNA with different abundances before and after enrichment by nano-hunter. (B) The ratio of the mutant peak before and after enrichment by nano-hunter. (C) Changes of mutation peak of 1% mtDNA with the increase of nano-hunter concentration.

1%, respectively, before the nano-hunter was added. After incubation at 32 °C, the mixture was ultrafiltered *via* an ultrafiltration spin column with a molecular weight cut-off of 100 kD. The filtrate at the bottom of the column was analyzed *via* PCR. We then sequenced the PCR products using Sanger sequencing to test for any signal changes at the mutation sites before and after nano-hunter capture. The sequencing results are shown in Fig. 2B. Compared with that in the control group, which did not contain the nano-hunter, significant incremental mtDNA enrichment (T > C) was observed in the group containing the nano-hunter. Fig. 2C shows the measurements and statistics of mtDNA signals, with "Input" representing the "Without nano-hunter" group and "Output" representing the "With nano-hunter" group. The mtDNA signal was detected after enrichment with the nano-hunter even when the abundance of mtDNA was lower than the detection limit of the Sanger sequencing method (~10%). These results demonstrated that the nano-hunter was successfully assembled and capable of capturing wtDNA, thus improving the abundance of mtDNA. Therefore, this nano-hunter may have significant advantages for the enrichment of low-abundance point mutations.

Then we aimed to verify the universality of mtDNA enrichment *via* nano-hunters. We selected the phosphatase and tensin homolog deleted on chromosome ten [*PTEN* R130Q (389G > A)] gene for further experiments. Similar to the results of the prior experiment, the nano-hunter bound to PTEN wtDNA and enriched mtDNA at abundances of 10% and 1% (Figs. 3A and B). Furthermore, even when the abundance of mtDNA was as low as 0.1%, the sample still generated an mtDNA signal when analyzed by Sanger sequencing after enrichment with the nano-hunter. Fig. 3C shows that the mtDNA signal peak intensity increased with increasing nano-hunter concentration, further demonstrating the functional success of the nano-hunter.

In the methods for enriching low-abundance point mutations, we believe that removal of wtDNA is performed more successfully than capture of mtDNA. The latter requires further separation of mtDNA from the capture tool after the capturing process, which increases the number of experimental steps and may also cause substantial mtDNA loss [16,18–20]. The enrichment mechanism of our newly developed nano-hunter is removal of wtDNA. Besides, the preparation of the nano-hunter was simple and efficient, and it was composed entirely of DNA, enabling better targeting and specificity for DNA sequences than other materials. Most importantly, the nano-hunter was also resettable, meaning that the nano-hunter used to enrich the mtDNA of gene *A* could be converted into another nano-hunter capable of enriching the mtDNA of gene *B*. Since there are many kinds of point mutations, methods that can be reset and reused for treating different targeting mutations would be highly preferred. The nano-hunter only consists of DNA strands, therefore it can easily realize resetting and reusing.

Fig. 4A illustrates the principle of resettability. The nano-hunter used for *BRCA1* mtDNA enrichment was reset for *PTEN* mtDNA enrichment *via* only three simple processes: addition of the complementary strands of hands for *BRCA1*, addition of the hands for *PTEN* and purification. Fig. 4B illustrates that the wtDNA of *BRCA1* was successfully captured before the nano-hunter was reset (after incubation of the wtDNA with the nano-hunter, ultrafiltration, and qPCR analysis of the filtrate, a significant reduction in the amount of *BRCA1* wtDNA in the filtrate was observed (red column). After resetting the nano-hunter, the filtrate from the nano-hunter treatment group exhibited only a slight decrease in the

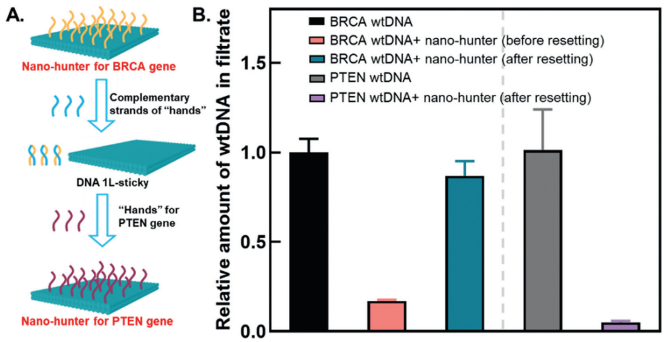

Fig. 4. Verification of nano-hunter resettability. The verification for the resettability of nano-hunter. (A) Schematic diagram of resettability verification of nano-hunter. (B) The capture efficiency of nano-hunter for *BRCA1* wtDNA and *PTEN* wtDNA before and after the resetting nano-hunter. Red column: the amount of *BRCA1* wtDNA remaining in the filtrate after incubation and ultrafiltration with nano-hunter before resetting nano-hunter; Blue column: the amount of *BRCA1* wtDNA remaining in the filtrate after incubation and ultrafiltration with nano-hunter after resetting nano-hunter; Purple column: the amount of *PTEN* wtDNA remaining in the filtrate after incubation and ultrafiltration with nano-hunter after resetting nano-hunter. Data are represented as mean ± SD, $n = 3$.

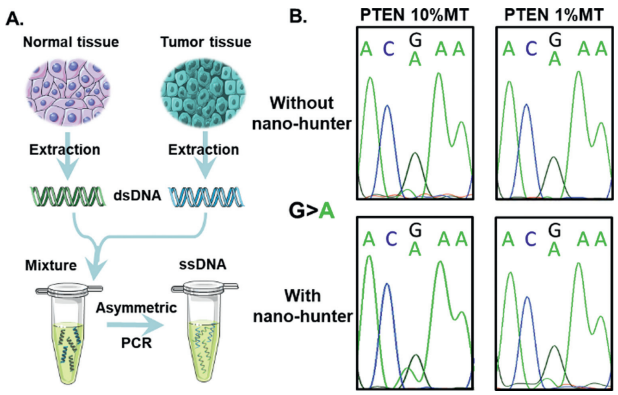

Fig. 5. Enrichment of clinical sample with *PTEN* R130Q (389G > A) gene by nano-hunter. (A) Schematic diagram of clinical sample preparation. (B) The sequencing peaks of mtDNA with different abundances from clinical samples before and after enrichment by nano-hunter.

amount of *BRCA1* wtDNA (blue column) and a significant decrease in the amount of *PTEN* wtDNA (purple column). Therefore, *via* a few simple processes, we were able to "format" the nano-hunter and "reload" it as a new nano-hunter, analogous to the formatting of a compact disc. This property may be unique to our enrichment materials and methods.

All the above experiments were performed using synthetic single-stranded DNA (ssDNA). However, clinical detection involves a double-stranded genomic DNA analyte. Therefore, we combined our method with PCR to enrich the mtDNA in clinical samples. *PTEN* mtDNA and wtDNA were extracted from formalin-soaked samples of endometrial carcinoma and normal tissues, respectively [9]. Next, we amplified the target fragment by PCR and used genomic wtDNA to dilute the genomic mtDNA [*PTEN* R130Q (389G > A) in endometrial carcinoma tissue], yielding samples with different abundances of mtDNA (50%, 10%, 1%, 0.1% and 0%). The extracted DNA samples were amplified by asymmetric PCR to generate ssDNA (Fig. 5A). The abundance of mtDNA in the 50%, 10% and 1% groups was significantly increased after treatment with the nano-hunter, suggesting that this method was also applicable to clinical samples (Fig. 5B and Table S2 in Supporting information).

In this work, DNA origami was applied to enrichment of cancer-related low-abundance point mutations. A nano-hunter was constructed using DNA origami, and hundreds of "hands" were installed on the surface of nano-hunter through DNA self-assembly. This novel enrichment method based on DNA nano-hunters eliminated DNA interference by using sample pretreatment before PCR amplification, and improve the abundance of the detection target—mtDNA. In addition, the nano-hunter was wholly composed of DNA strands, thus minimizing non-specific removal of the target DNA. This method was also advantageous due to its simplicity, short experimental period, and resettability. Compared with the fluorescent probe and PCR method, this strategy enriches the mutant target in a lower wild-type background. The system is resettable and universal as well, and its optimization process is economical.

In the future, optimizing the system parameters and choosing the more sensitive method to detect the target after enrichment will further improve the property of this method. The applications of toehold-mediated strand displacement reaction and temperature-dependent chain hybridization will allow nano-hunters to be more easily recycled than other enrichment materials [32,33]. More importantly, the structure of DNA origami is highly flexible and modifiable. Multiple modifications to the DNA origami substrate can greatly enhance the function of DNA nanorobots. For example, assembling multiple hands that can capture different target genes would allow a single nano-hunter to simultaneously enrich different point mutations, significantly improving the experimental efficiency. The novel DNA nano-hunter designed in our study may serve as a valuable tool for the enrichment and detection of tumor markers, potentially enabling early cancer diagnosis.

Declaration of competing interest

The authors declare that they have no known competing financial interests or personal relationships that could have appeared to influence the work reported in this paper.

Acknowledgments

This research was funded by the National Key R&D Program of China (Nos. 2018YFA0903500, 2018YFC0114600), the National Natural Science Foundation of China (Nos. 51703073, 22077042), the Fundamental Research Funds for the Central University (No. 2021yjsCXCY114, China).

References

[1] L.A. Loeb, Nat. Rev. Cancer 11 (2011) 450–457.
[2] L. Ding, G. Getz, D.A. Wheeler, et al., Nature 455 (2008) 1069–1075.
[3] D. Bell, A. Berchuck, M. Birrer, et al., Nature 474 (2011) 609–615.
[4] S. Nik-Zainal, P. Van Loo, D.C. Wedge, et al., Cell 149 (2012) 994–1007.
[5] T.B. Wu, X.J. Xiao, Z. Zhang, et al., Chem. Sci. 6 (2015) 1206–1211.
[6] M.A. Chapman, M.S. Lawrence, J.J. Keats, et al., Nature 471 (2011) 467–472.
[7] S.L. Carter, K. Cibulskis, E. Helman, et al., Nat. Biotechnol. 30 (2012) 413–421.
[8] N. Liu, X.Z. Zhang, X.F. Tang, et al., Chem. Commun. 56 (2020) 14397–14400.
[9] X.F. Tang, N. Chen, R.J. Liu, et al., Anal. Chim. Acta 1134 (2020) 28–33.
[10] X.J. Xiao, T.B. Wu, L. Xu, et al., Nucleic Acids Res. 45 (2017) e90.
[11] S. Maman, I.P. Witz, Nat. Rev. Cancer 18 (2018) 359–376.
[12] Y. Zhou, G.A. Abel, W. Hamilton, et al., Nat. Rev. Clin. Oncol. 14 (2017) 45–56.
[13] N.E. Broude, L.G. Zhang, K. Woodward, et al., Proc. Natl. Acad. Sci. U. S. A. 98 (2001) 206–211.
[14] J. Li, L.L. Wang, H. Mamon, et al., Nat. Med. 14 (2008) 579–584.
[15] C.A. Milbury, M. Correll, J. Quackenbush, et al., Clin. Chem. 58 (2012) 580–589.
[16] J. Tost, Expert Rev. Mol. Diagn. 16 (2016) 265–268.
[17] H.Y. Wang, J. Jiang, B. Mostert, et al., J. Mol. Diagn. 15 (2013) 62–69.
[18] M. Guha, E. Castellanos-Rizaldos, P. Liu, et al., Nucleic Acids Res. 41 (2013) e50.
[19] J. Lee, H. Lim, H. Jang, et al., Nucleic Acids Res. 47 (2019) e1.
[20] C. Song, Y. Liu, R. Fontana, et al., Nucleic Acids Res. 44 (2016) e146.
[21] T. Chen, L. Ren, X. Liu, et al., Int. J. Mol. Sci. 19 (2018) 1671.
[22] D. Yang, M.R. Hartman, T.L. Derrien, et al., Acc. Chem. Res. 47 (2014) 1902–1911.
[23] P.W.K. Rothemund, Nature 440 (2006) 297–302.
[24] M. Madsen, K.V. Gothelf, Chem. Rev. 119 (2019) 6384–6458.
[25] S. Dey, C. Fan, K.V. Gothelf, et al., Nat. Rev. Methods Primers 1 (2021) 13.

[26] S.M. Douglas, I. Bachelet, G.M. Church, Science 335 (2012) 831–834.
[27] S.P. Li, Q. Jiang, S.L. Liu, et al., Nat. Biotechnol. 36 (2018) 258–264.
[28] L.X. Cheng, Z.K. Zhang, D. Zuo, et al., ACS Appl. Mater. Interfaces 10 (2018) 34869–34877.
[29] Y. Tokura, Y.Y. Jiang, A. Welle, et al., Angew. Chem. Int. Ed. 55 (2016) 5692–5697.
[30] Y. Tokura, S. Harvey, C.J. Chen, et al., Angew. Chem. Int. Ed. 57 (2018) 1587–1591.
[31] S. Wu, M. Zhang, J. Song, et al., ACS Nano 15 (2021) 1555–1565.
[32] L. Li, W. Zhang, X. Tang, et al., Chem. Commun. 56 (2020) 8794–8797.
[33] F.C. Simmel, B. Yurke, H.R. Singh, Chem. Rev. 119 (2019) 6326–6369.